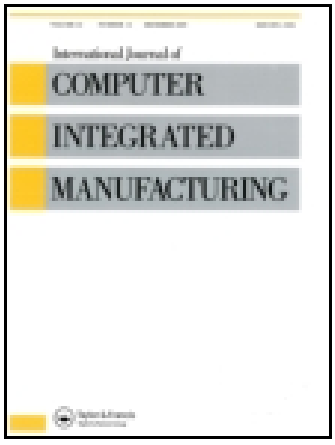

International Journal of Computer Integrated Manufacturing

Publication details, including instructions for authors and subscription information:
http://www.tandfonline.com/loi/tcim20

Visual inspection of glass bottlenecks by multiple-view analysis

Miguel Carrasco [a], Luis Pizarro [a b c] & Domingo Mery [d]

[a] Escuela de Ingeniería Informática, Facultad de Ingeniería, Universidad Diego Portales, Santiago, Chile

[b] Mathematical Image Analysis Group, Faculty of Mathematics and Computer Science, Saarland University, Saarbrücken, Germany

[c] Department of Computing, Imperial College London, 180 Queen's Gate, London, SW7 2AZ, UK

[d] Departamento de Ciencia de la Computación, Pontificia Universidad Católica de Chile, Santiago, Chile

Published online: 22 Sep 2010.

To cite this article: Miguel Carrasco, Luis Pizarro & Domingo Mery (2010) Visual inspection of glass bottlenecks by multiple-view analysis, International Journal of Computer Integrated Manufacturing, 23:10, 925-941, DOI: 10.1080/0951192X.2010.500676

To link to this article: http://dx.doi.org/10.1080/0951192X.2010.500676

International Journal of Computer Integrated Manufacturing
Vol. 23, No. 10, October 2010, 925–941

Taylor & Francis
Taylor & Francis Group

Visual inspection of glass bottlenecks by multiple-view analysis

Miguel Carrasco[a]*, Luis Pizarro[a,b,c] and Domingo Mery[d]

[a]*Escuela de Ingeniería Informática, Facultad de Ingeniería, Universidad Diego Portales, Santiago, Chile;* [b]*Mathematical Image Analysis Group, Faculty of Mathematics and Computer Science, Saarland University, Saarbrücken, Germany;* [c]*Department of Computing, Imperial College London, 180 Queen's Gate, London, SW7 2AZ, UK;* [d]*Departamento de Ciencia de la Computación, Pontificia Universidad Católica de Chile, Santiago, Chile*

(*Received 14 September 2009; final version received 6 June 2010*)

The narrow structure of bottlenecks poses a very challenging problem for automated visual inspection systems and surprisingly, this issue has received little attention in literature. Bottleneck inspection is highly relevant to the fabrication of glass bottles, e.g., for the wine and beer industry. Defects in glass bottles can arise in various situations such as an incomplete reaction in a batch, batch contaminants and interactions of the melted material among others. This paper presents an inspection approach that utilises geometry of multiple views along with a rich set of feature descriptors to discriminate real flaws from false alarms in uncalibrated images of glass bottlenecks. The proposed method is based on an automatic multiple view inspection (AMVI) technique for the automatic detection of flaws. This technique involves an initial step that extracts numerous segmented regions from a set of views of the object under inspection. These regions are subsequently classified either as real flaws or as false alarms. The classification process considers that image noise and false alarms occur as random events in different views while real flaws induce geometric and featural relations in the views where they appear. Therefore, by analysing such relations it is possible to successfully localise real flaws and to discard a large number of false alarms. An important characteristic of the proposed methodology is the complete lack of camera calibration which makes our method very suitable for applications where camera calibration is difficult or expensive to carry out. Our inspection system achieves a *true positive rate* of 99.1% and a *false positive rate* of 0.9%.

Keywords: automated visual inspection; flaw detection; multiple views; uncalibrated images; glass bottlenecks

1. Introduction

Visual inspection is defined as a quality control task that determines if a product deviates from a given set of specifications using visual data (Malamas *et al.* 2003), (Kumar 2008). Inspection usually involves measurements of specific parts features such as assembly integrity, surface finish and geometric dimensions. If the measurements lie within a determined tolerance, the inspection process deems the product acceptable for use. In industrial environments, inspection is generally performed by human inspectors during different phases of the production process. The economic benefits of employing human inspectors is one of the deciding factors for companies when developing their production process. The investment cost to install and develop a specialised machine for inspection tasks is very high compared to the cost of training a human operator. Human inspectors do have some major drawbacks, they are not always consistent and effective evaluators because the inspection tasks are monotonous and exhausting (Mital *et al.* 1998). Typically, a human inspector only rejects one out of hundreds of accepted products. According to Drury *et al.* (2004), human inspection is at best 80% effective. Achieving 100% effectiveness would require a high level of redundant testing, meaning several human control points, which naturally increases costs and slows down the inspection task and subsequent manufacturing processes (Jacob 2004). Human visual inspection has been estimated to account for at least 10% of total fabrication costs. In some applications, it suffices to select a reduced but representative set of products to inspect, from which statistical inference is applied to estimate the amount of defective products in the total production. Nevertheless, there are existing applications which require every product to be inspected thoroughly, i.e., an inspection process needs to be 100% effective. All of these factors have lead the industry gradually to replace human inspection with automatic visual inspection (AVI) methods which allow for contact free inspections.

Since the introduction of AVI methods in the early 1980s (Jarvis 1980, Chin and Harlow 1982) several systems for quality inspection have been successfully developed using different image processing techniques. The main objective of AVI is to increase productivity

*Corresponding author. Email: miguel.carrasco@mail.udp.cl

ISSN 0951-192X print/ISSN 1362-3052 online

DOI: 10.1080/0951192X.2010.500676
http://www.informaworld.com

while ensuring high quality, reliability and consistency standards, i.e., rejecting most of the defective products and accepting all of the defect-free products. Despite their advantages, AVI methods in general also have the following problems. 1) They lack precision in their performance because of the imbalance between undetected flaws (false negatives) and false alarms (false positives). 2) They are limited by time, the mechanical requirements for placing an object in the desired position can be time consuming. 3) They have high computing costs when determining whether the object is defective or not. 4) They generate high complexity configurations and lack flexibility for analysing changes in parts design. The issues outlined above show that AVI still contains some problem areas and can benefit from the development of new applications.

The wine and beer industry requires the fabrication of flawless glass bottles. Defects in glass bottles can arise in various situations such as an incomplete batch reaction, batch contaminants which fail to melt completely, interactions of the melted material with glass-contact refractories and superstructure refractories as well as by devitrification. If abnormal conditions arise, multiple flaws can occur and even one flaw of only 1–2 mg in every 100 mg article can be enough to produce 100% rejection rates (Parker 2000). Most of the methods proposed in literature for automated glass bottle inspection attempt to identify flaws in the lips, body and bottom of the bottles, e.g. Canivet *et al.* (1994), Firmin *et al.* (1997), Hamad (1998), Ma *et al.* (2002), Shafait *et al.* (2004), Wang *et al.* (2005), Yan and Cui (2006), Duan *et al.* (2007), Yepeng *et al.* (2007) and Katayama *et al.* (2008). Very few of those investigations deal with the problem of detecting flaws in the bottleneck (Ma *et al.* 2002, Mery and Medina 2004). The bottleneck makes the inspection task very challenging owing to its narrow and difficult to manipulate structure. Even the smallest undetected flaw around this region can cause grave danger for consumers. For example, the introduction of the cork into a wine bottle could detach glass particles from a defective region posing a threat of ingestion. Encouraged by the opportunity for advancement in this area, this investigation focuses on inspection of necks in empty glass bottles.

We can classify bottle inspection systems into two categories: approaches that make use of a single view/camera for detecting flaws, e.g. Canivet *et al.* (1994), Mery and Medina (2004), Wang and Duan (2005), Yan and Cui (2006), Duan *et al.* (2007) and Yepeng *et al.* (2007) and frameworks utilising multiple views/cameras to reinforce the detection process, e.g. Firmin *et al.* (1997), Hamad (1998), Ma *et al.* (2002), Shafait *et al.* (2004) and Katayama *et al.* (2008). This investigation employs a single camera for image acquisition. However, it captures multiple views of the bottleneck, taken at successive rotations of the bottle along its principal axis, i.e., recording an image sequence of the bottleneck.

In order to detect the flaws, a novel methodology that tracks potential flaws along the acquired image sequence was implemented. The key observation is that only real flaws can be successfully tracked, since they do induce spatial relations between the views where they appear. Conversely, potential flaws that cannot be tracked will be considered as false alarms. This idea was originally proposed for flaw detection in calibrated X-ray images (Mery and Filbert 2002). This paper extends that approach to the analysis of uncalibrated image sequences. Moreover, the combination of geometry of multiple views and several feature descriptors is used to achieve a precise distinction between real flaws and false alarms. This paper also extends previous ideas presented in Carrasco and Mery (2006), Pizarro *et al.* (2008), Carrasco and Mery (2010).

The paper is organised as follows. Section 2 presents a prototype for image acquisition of glass bottlenecks. Section 3 describes the inspection algorithm for tracking real flaws in multiple views. Section 4 reports on the performance achieved by the inspection system in comparison with other methods proposed in previous works. Finally, Section 5 summarises the paper's contributions and succinctly describes some ongoing and future work.

2. Electro-mechanical system for image sequence acquisition

The lighting selection for an inspection system is crucial. Since natural lighting conditions are dynamic and change all the time it is not feasible to implement algorithms that are robust to illumination changes without burning important computational time (Kumar 2008). Therefore, artificial lighting is required to achieve adequate and uniform illumination for real-time inspection systems. There are several existing studies, e.g. Vazquez (2007) and Marchand (2007), concerning the placement of external light sources around the object under examination. However, none of these studies have developed an internal illumination system that can be effectively applied to the detection of flaws in glass bottles. This paper proposes the design of an electro-mechanical device for image acquisition and inspection of glass bottlenecks using an internal illumination system.

Figure 1(a) displays the electro-mechanical device for image sequence acquisition holding an empty glass bottle. A close-up around the bottleneck (Figure l(b)) shows the illuminating tube placed inside the bottle.

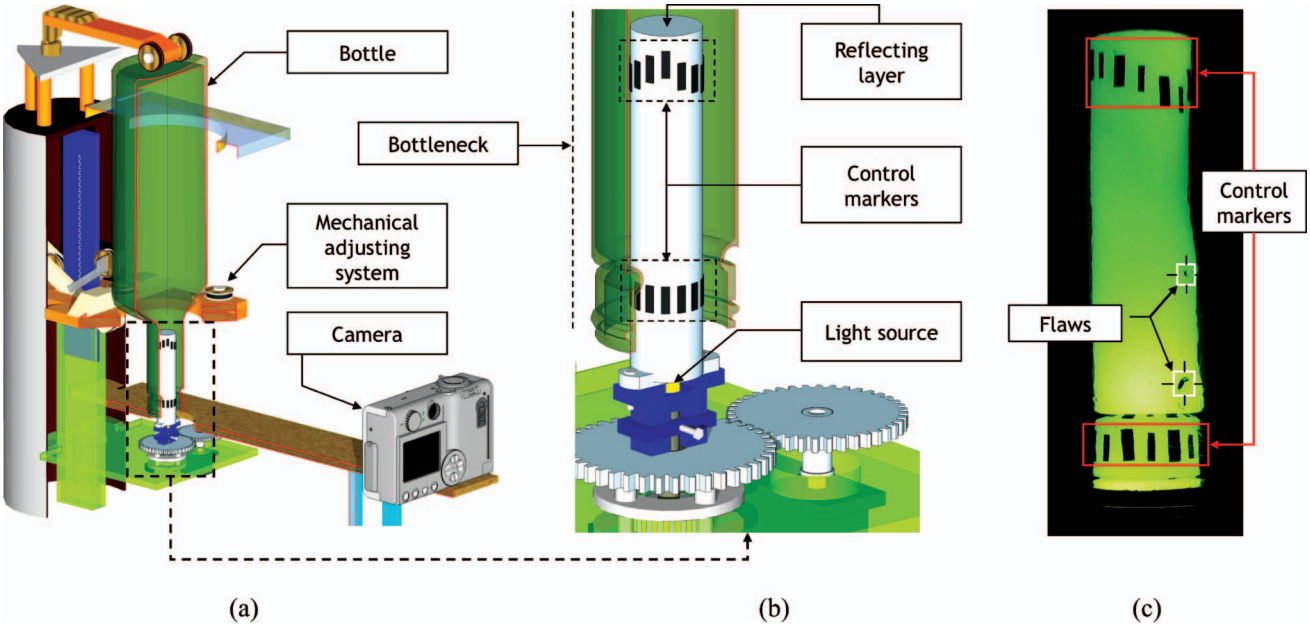

Figure 1. (a) Proposed electro-mechanical prototype for image acquisition; (b) details of the illuminating tube; (c) example of an image captured by the CCD camera.

Four LEDs (T1 3.5v-20mA) emitting uniform white light are located at the bottom of the tube. To improve light uniformity a reflecting layer has been fixed at the other extreme of the tube. This way the definition of the acquired images improves greatly, which increases the probability of capturing even the smallest flaws around the bottleneck, and intrinsic reflections owing to external light sources are avoided.

To the best of the authors' knowledge, there are no existing inspection systems for glass bottles which use an internal illumination system. In this system no additional light sources are used apart from the illuminating tube. Another important characteristic of the illuminating tube is the set of control markers situated at both extremes. As later described in Section 3.2, the control markers allow for computational accuracy in corresponding points between different views, which is a fundamental step for detecting flaws in multiple views. Figure 1(c) shows an image, taken by a standard CCD camera, that contains two highlighted flaws.

The proposed system can detect flaws more efficiently by looking at several images of the object under inspection. Therefore, the image acquisition system needs to be able to capture, with only one camera, multiple images taken from different viewpoints. To achieve this, the prototype has an electro-mechanical system (Figure 2) that simultaneously rotates the bottle and the illuminating tube at configurable spin angles that are controlled by a step motor. An image sequence of the bottleneck is then taken at successive rotations of the glass bottle. The experimental prototype uses a Canon S3 IS camera with resolution 2592×1944 pixels and a dynamic range of 24 bits. The camera is placed about 20 cm from the bottleneck. The device also includes a mechanical adjusting system to adapt inspection for different bottleneck lengths. An adjustable arm holds the bottle from its body while a press mechanism pushes the bottle against the axle to maintain its vertical position.

The electro-mechanical system is manipulated by a Basic Stamp micro-controller PIC16C57 connected to a standard personal computer via a RS232 communication port. The micro-controller is programmed in Pbasic (Martin 2005). For a specified spin angle α (in degrees) the micro-controller synchronises the step motor with the illumination system. The camera's acquisition process is triggered by a control system via Matlab. The image sequence consists of $\lfloor 360/\alpha \rfloor$ different views, where $\lfloor \cdot \rfloor$ is the floor function.

The prototype was built considering an upside down bottle similar to Wang and Asundi (2000), but it is also possible to assemble the system with the bottle right side up. Note that in contrast to several inspection systems that make use of multiple cameras (Firmin *et al.* 1997, Hamad 1998, Ma *et al.* 2002, Shafait *et al.* 2004, Katayama *et al.* 2008) the proposed inspection mechanism only employs a single camera. This simplifies the scene's geometry and suffices to build a robust flaw detection system by analysing the acquired image sequence. It is important to mention that no camera calibration procedure is considered

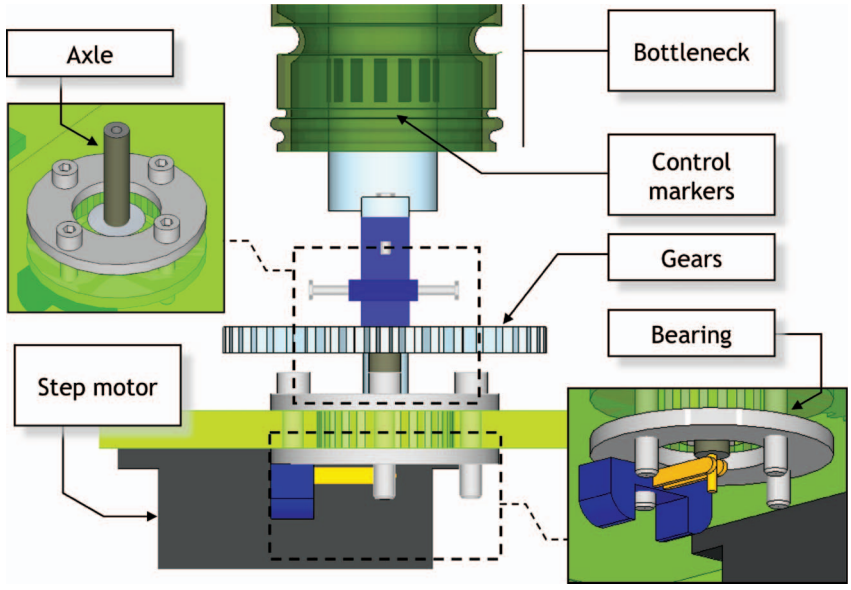

Figure 2. Mechanical system that simultaneously rotates the bottle and the illuminating tube.

at all. (We refer to Carrasco and Mery (2010) for further discussion about the calibration problem in industrial environments.) In the next section we focus on the flaw detection process in uncalibrated image sequences.

3. Inspection system for flaw detection in uncalibrated images

Motivated by (human) visual inspections that are able to differentiate between flaws and noise, by looking at the objects being tested in motion, a method of automated inspection was developed using sequences of multiple images (Mery and Filbert 2002) called *Automated Multiple View Inspection* (AMVI). The AMVI methodology uses redundant views to perform the inspection task. The main idea is to consider as false alarms those potential flaws that cannot be tracked in a sequence of multiple images. Although, in some applications a unique image might be enough for inspecting certain objects or materials, the use of multiple views of the same object taken from different viewpoints can be used to confirm and improve the diagnosis made by analysing only one image. Normally, the main problem when dealing with flaw segmentation in low signal-to-noise ratio image systems is the appearance of numerous false alarms. These systems use only one view when separating real flaws and false alarms. AMVI methodology differs greatly and proposes that an augmentation in the number of views can reduce the number of false alarms as well as conserve the majority of real flaws owing to the redundancy of information.

Some of the main advantages of AMVI inspection of objects are: (1) characterise with greater precision their physical properties by providing more visual information; (2) increase performance in the detection and classification of surface defects, visible in light, or internal structural defects with X-rays using a geometric classification scheme; (3) reduce the number of false alarms by utilising the redundancy of visual information; and (4) model the object's motion by means of a geometric analysis, which allows modelling the whole structure of the object internally and/or externally. Nowadays, AMVI methodology can be applied not only to the inspection of objects such as tire rims, bottles or welds, but also to the inspection of food, airport surveillance and security.

This investigation aims to exploit the redundant information contained in the bottleneck's multiple views to accurately detect real flaws and discard false alarms. As mentioned before, only real flaws induce geometric and featural relations in multiple views, while noise and false alarms appear as random events. Geometric characteristics in uncalibrated images are established by both bifocal and trifocal analysis of multiple views (Hartley and Zisserman 2000) whereas the featural characteristics are extracted by several feature descriptors proposed in previous investigations. Potential flaws that match this set of characteristics in multiple views are thus regarded as real flaws. This can also be seen as a tracking process because the image sequence, obtained from successive rotations of the bottle, is analysed and the system only classifies as real flaws those that can be tracked along the whole sequence.

Considering the aspects mentioned above, this paper proposes a three-step methodology to flaw detection in bottlenecks: (a) segmentation and feature extraction of potential flaws, (b) computation of corresponding points between views, and (c) tracking flaws in multiple views. Figure 3 shows a general overview of the proposed approach for image acquisition and inspection of glass bottlenecks. The following sections explain each step in further detail.

3.1. *Segmentation and feature extraction of potential flaws*

In previous investigations there are a large number of segmentation algorithms designed to detect surface

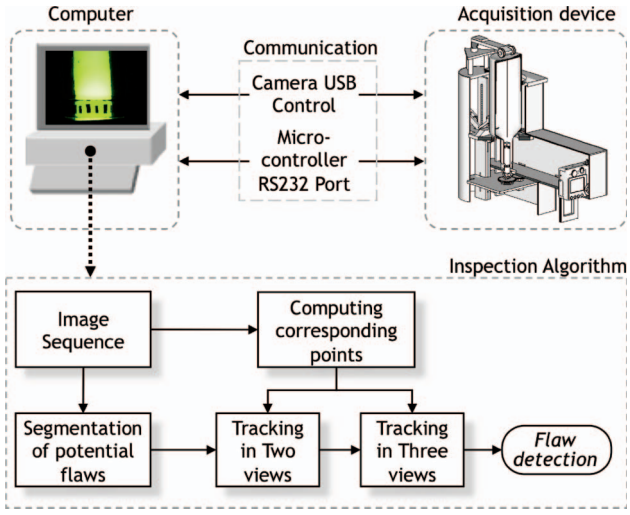

Figure 3. Proposed system for image acquisition and inspection of glass.

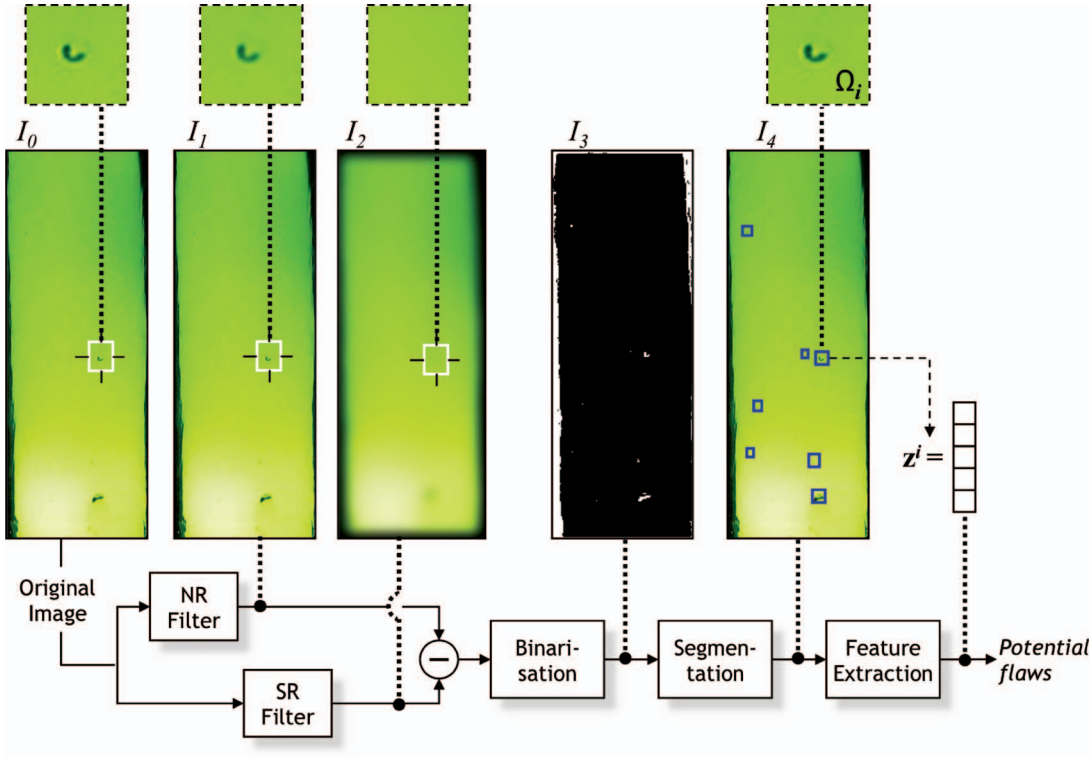

Figure 4. Segmentation and feature extraction of potential flaws.

flaws or defects after a classification process, e.g. Chung and Kim (1998), Mamic and Bennammoun (2000), Liao (2003), Shafait (2004) and Linhari and Obac (2005). However, those methods normally use an image to verify if a potential flaw is an actual flaw and not a false alarm. This paper carries out the classification process by means of incremental multiple views analysis. At this stage each image of the sequence is processed independently in order to segment multiple potential flaws, and later those multiple segmented regions are combined. The procedure outlined in Figure 4 is as follows: Each image I_0 of the sequence is pre-processed by two independent filters. A *noise removal* (NR) filter is used to reduce the amount of noise intrinsic to any CCD sensor. A Gaussian filter with fixed kernel size 3×3, obtains a filtered image I_1. A *structure removal* (SR) Gaussian filter with kernel size (Gaussian filtering is efficiently computed with large spatial supports using the Fast Fourier Transform (FFT)) $n \times n$, $n \gg 3$, is used to blur any structure present in the image and obtain a uniform background image I_2. Subsequently, the absolute difference $|I_1 - I_2|$ is binarised using the *valley-emphasis* method (Hui-Fuang 2006), obtaining an image mask I_3 with potential flaws. Finally, for each potential flaw segmented in a region Ω_i a set of features are computed and stored in a feature vector $\mathbf{z}^i$, as shown in the image I_4. Table 1 describes the numerous feature descriptors for grey-scale and colour images employed in this study. Section 3.3 details how potential flaws are tracked in two and three different views by matching their feature vectors. The tracking task itself can be highly demanding due to the possibly large number of potential flaws generated by segmentation, though only a few might correspond to real flaws. To maximise the probability of capturing all real flaws the segmentation process is tuned by the kernel size parameter n. Later on the experimental section discusses the effect of varying n as well as the performance of each feature descriptor in the flaw tracking process.

Table 1. Different feature descriptors we employ to characterise the segmented potential flaws.

Descriptor	Notes
HU	(Hu 1962) proposed a descriptor composed by seven moments invariant under scale, rotation, translation and skew transformations.
Co-occurrence	(Haralick *et al.* 1973) introduced a descriptor based on the computation of the co-occurrence matrix. We compute it for the contrast, homogeneity and energy of each colour channel (Castleman 1996).
FSK (A)	(Flusser and Suk 1993) proposed a set of moments invariant under affine geometric transformations.
FSKS (B)	(Flusser *et al.* 1996) designed a set of moments invariant under motion blur.
FSKS (B + S)	(Flusser *et al.* 1996) extended the FSKS (B) moments by introducing 4 new moments invariant under scale and rotational transformation.
CLP	(Mery 2003) proposed the *crossing line profiles* (CLP) descriptor whose features correspond to the first five harmonics of the fast Fourier transform.
PSO*	(Mindru 2004) introduced a descriptor invariant under photometric transformations of scale and translation (robust to illuminations changes).
GPSO	(Mindru 2004) extended the PSO* descriptor by including invariants under affine geometric deformations.
GPD	(Mindru 2004) proposed another descriptor invariant under diagonal photometric and geometric transformations.
SIFT	(Lowe 2004) introduced a descriptor invariant under scale and rotation transformations and partially invariant to illumination changes.
PHOG	(Bosch and Zisserman 2007) proposed a descriptor based on a vectorial representation of the spatial distribution of edges.
SURF	(Bay 2008) introduced a descriptor invariant under scale and rotation transformations.

3.2. Computation of corresponding points between views

The geometric relations between potential flaws in different views can be described by sound mathematical concepts from *multiple view geometry* (Hartley and Zisserman 2000). In particular, it is possible to relate points in two and three views via the *so-called* bifocal and trifocal analysis, respectively. The next section develops such analysis. In order to compute these geometric relations it is necessary to have accurate corresponding points between the views. Such points will later allow for matching of potential flaws along the bottleneck's image sequence.

Corresponding points are found easily by placing equidistant control markers on both extremes of the illumination source (Figure 1(b)). The mass centre of these markers is known since they were also extracted in the previous segmentation step. The lower control markers are positioned at the same vertical level, while the upper ones follow a sinusoidal wave. Using these markers, it is possible to compute a set of corresponding points between each pair of consecutive or non-consecutive views. This is schematically outlined in Figure 5. The upper and lower control markers of each view are connected through vertical lines between their

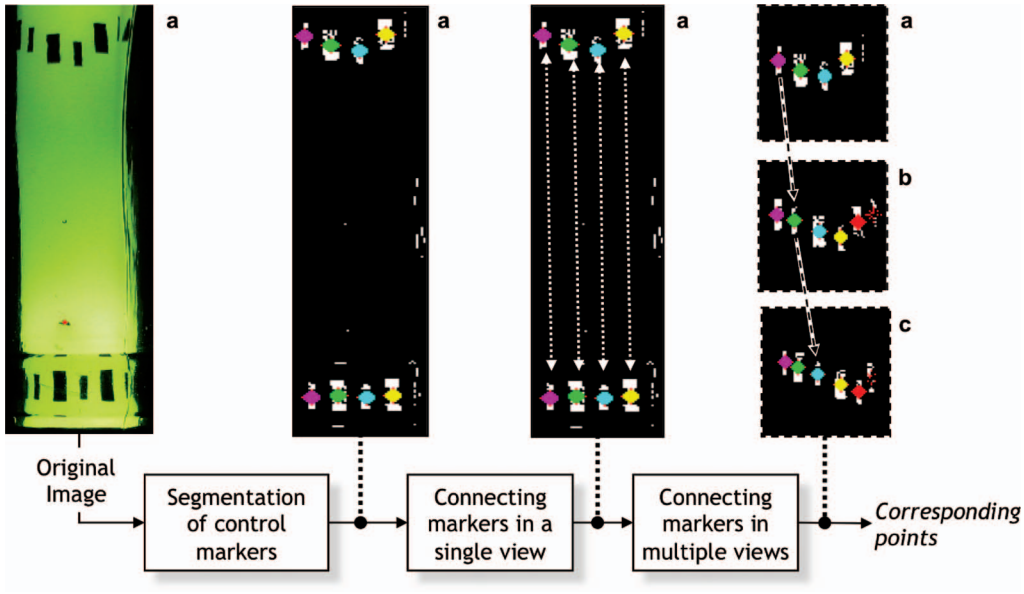

Figure 5. Computation of corresponding points in two and three views *a*, *b* and *c*.

mass centre. Since the length of a vertical line connecting two particular markers remains constant along the image sequence, the relative position of these markers in different views is known. Therefore, the set of corresponding points between two or three views is conformed by the relative positions of their markers. Section 3.3 employs such correspondences to establish geometric relations between potential flaws in two and three views.

3.3. *Tracking flaws in multiple views*

After having segmented and extracted features for all potential flaws in an image sequence, and having computed a set of corresponding points between every pair of images, the investigation now turns to the problem of separating real flaws from false alarms. This goal is achieved by performing tracking of the potential flaws in two and in three views. Only real flaws can be tracked along multiple views, since they do induce geometric and featural relations in the different views where they appear, while false alarms correspond to random events. The tracking processes in two and three views are detailed below.

Tracking in two views

In the following it is considered that the mass centre of the potential flaw i in view a is stored in homogenous coordinates as $\mathbf{m}_a^i = [x_a^i, y_a^i, 1]^{\mathrm{T}}$. If this potential flaw is actually a real flaw it must have a corresponding point $\mathbf{m}_b^j$ in another (non-) consecutive view b where a potential flaw j was also segmented. According to the *principle of multiple view geometry* (Hartley and Zisserman 2000), the points $\mathbf{m}_a^i$ and $\mathbf{m}_b^j$ correspond to each other if they are related by the *fundamental matrix* $\mathbf{F}_{a,b}$ such that

$$\mathbf{m}_b^{j\,\mathrm{T}} \cdot \mathbf{F}_{a,b} \cdot \mathbf{m}_a^i = 0 \tag{1}$$

Note that the matrix $\mathbf{F}_{a,b}$ is known provided that it was estimated by the algorithm described in Chen (2000) using the correspondences found in Section 3.2. The relation (1) is known as *epipolar constraint*. It indicates that a corresponding point $\mathbf{m}_b^j$ can only lie on the epipolar line of point $\mathbf{m}_a^i$ defined as $\mathbf{l}_a^i = \mathbf{F}_{a,b} \cdot \mathbf{m}_a^i = [l_{a,x}^i, l_{a,y}^i, l_{a,z}^i]$. It is possible to have several points lying on the epipolar line as shown in Figure 6(a). In this case, the correspondence associated with $\mathbf{m}_a^i$ is identified as the point $\mathbf{m}_b^j$ that satisfies the following condition

$$\frac{\left|\mathbf{m}_b^{j\,\mathrm{T}} \cdot \mathbf{F}_{a,b} \cdot \mathbf{m}_a^i\right|}{\sqrt{(l_{a,x}^i)^2 + (l_{a,y}^i)^2}} < \varepsilon \tag{2}$$

for small $\varepsilon > 0$. That is, the point $\mathbf{m}_b^j$ with the smallest (perpendicular) distance to the epipolar line $\mathbf{l}_a^i$ is chosen. In this case, a geometric match has been found, which could be regarded as a real flaw with a bifocal relationship. However, it is important to emphasise that the condition (2) is not enough to ensure correct matches in two views. Figure 7 shows the different types of matches that can result:

(1) *one-to-one*: Figure 7(a) displays the case of only one possible geometric match for every

potential flaw, although it does not necessarily mean that every match is correct.

(2) *one-to-many*: Figure 7(b) exhibits a possible wrong match and a match that could not be established. The latter case occurs when condition (2) is not fulfilled.

(3) *many-to-one*: Figure 7(c) shows multiple matches to the same flaw in the second view.

This shows that purely geometric relations can lead to wrong matches. Such consequences are less favourable when there is a large number of false alarms and even worse when searching for correspondences in three views. As a remedy, the system analyses not only the geometric characteristics of the potential flaws but also their featural characteristics. This way the system can filter out most of the wrong matches outlined in Figure 7.

It is necessary to introduce a short notation to describe the feature analysis carried out. Let $\mathbf{z}_a^i$ and $\mathbf{z}_b^j$ be the feature vectors (see Section 3.1 and Figure 4) of the potential flaw i in the first view a and the potential flaw j in the second view b, respectively. The system then computes the Euclidean distance between both feature vectors as $d_{a,b}^{i,j} = \|\mathbf{z}_a^i - \mathbf{z}_b^j\|$, and defines the array $\mathbf{X}_{a,b}$ containing all possible geometric matches in both views and the vector $\mathbf{D}_{a,b}$ with the corresponding featural distances

index	$\mathbf{X}_{a,b}(index)$	$\mathbf{D}_{a,b}(index)$
1	$\{1,1\}$	$d_{a,b}^{1,1}$
	$\{i,j\}$	$d_{a,b}^{i,j}$
p	$\{n.m\}$	$d_{a,b}^{n,m}$

Now, given $\mathbf{X}_{a,b} \in Z^{p\times 2}$ and $\mathbf{D}_{a,b} \in \mathbf{R}^{p\times 1}$, the *nearest neighbour distance ratio* (NNDR) criterion is executed (Mikolajczyk 2004), described in Algorithm 1, to obtain the set of matches $\mathbf{X'}_{a,b} \in Z^{p\times 2}$ that minimise the featural distances among all possible matches (alternative criterion exist in literature, but NNDR was chosen because it is computationally inexpensive (see Sidibe *et al.* 2007)). As noted in

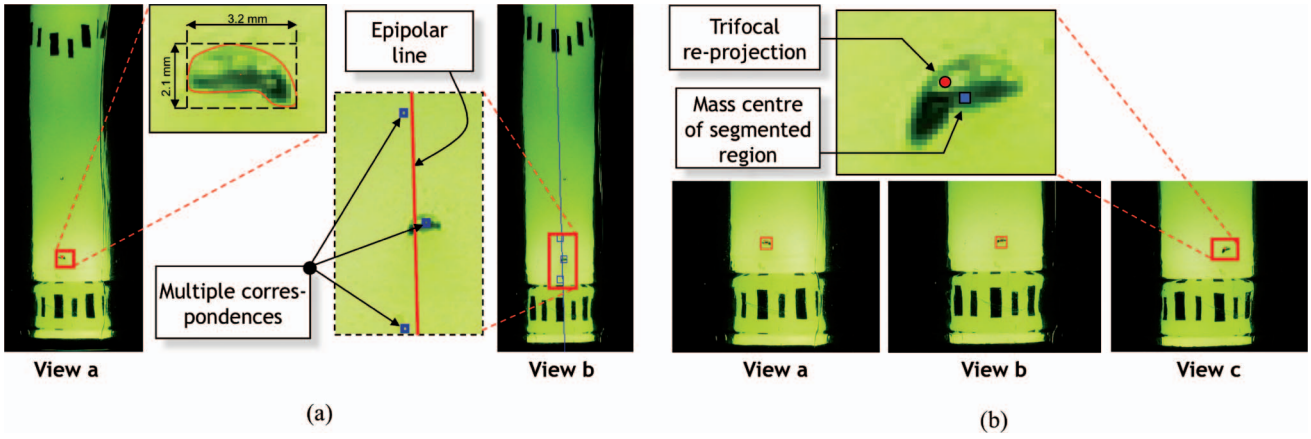

Figure 6. Examples of (a) bifocal and (b) trifocal correspondences.

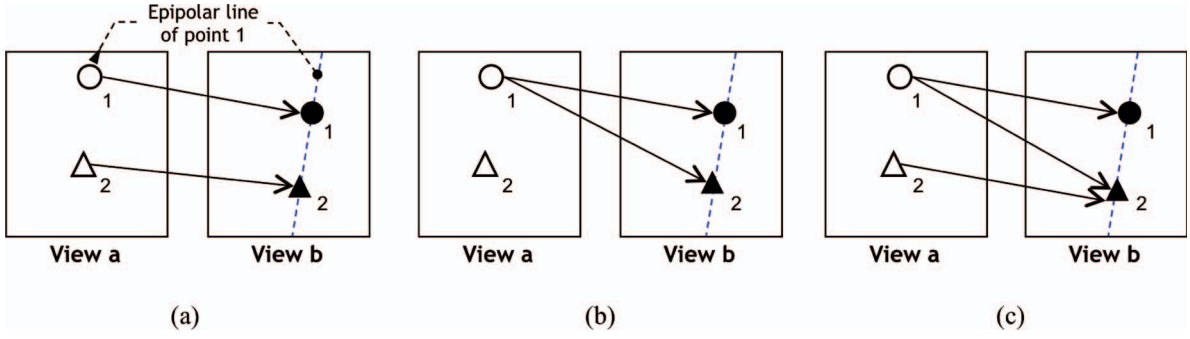

Figure 7. Possible geometric matches in two views. (a) Ideal *one-to-one* match, (b) *one-to-many* matches that can be resolved by the NNDR criterion, and (c) *many-to-one* matches that can be resolved by the proposed bNNDR criterion.

Algorithm 1, line 4, this criterion is useful to resolve matches which fall into the *one-to-many* category, as depicted in Figure 7(b). However, it fails to correct the wrong *many-to-one* matches shown in Figure 7(c).

To overcome this problem, the system introduces a novel and simple modification to the NNDR criterion that is able to resolve the general case of *many-to-many* matches. It is called *bidirectional* NNDR (bNNDR) criterion because it checks both the possible matches going from the first view a to the second view b (as in Algorithm 1 line 4) and those going from the second to the first view. By looking at both directions it is possible to adjust the distance feature vector $\mathbf{D}_{a,b}$ with a weighting vector $\mathbf{W}_{a,b} \in \mathbf{R}^{p\times 1}$. Algorithm 2 shows the computation of $\mathbf{W}_{a,b}$. The weights are set to 1 for *one-to-one* matches and for the matches with minimal *backward* distance, while matches with larger distances get weights larger than 1. In this way, the distance vector $\mathbf{D}_{a,b}$ is cross-correlated with information from all multiple matches. The proposed bNNDR criterion, fully described in Algorithm 3, outperforms the NDDR criterion in identifying the correct matches from sets of *many-to-many* matches, which will be demonstrated in the experimental section.

Tracking in three view

If the segmentation stage (Section 3.1) outputs a large number of potential flaws of small size, which might have very similar feature vectors, it is likely that the precedent two-view tracking process classifies matches that correspond to false alarms as real flaws. In order to avoid such a result, the system elaborates on a three-view tracking mechanism to discard wrong matches and to confirm those which do indeed represent real flaws. In terms of geometry of multiple views, given a potential flaw with corresponding coordinates $\mathbf{m}_a^i$ and $\mathbf{m}_b^j$ in the views a and b, one can estimate the hypothetical position of a third correspondence $\mathbf{m}_c^k$ in a view c by

Algorithm 1 : *Nearest neighbour distance ratio* (NNDR) criterion for two views a and b.

Input: $\mathbf{X}_{a,b}, \mathbf{D}_{a,b}$, and deflaw parameter $\sigma = 0.7$
Output: $\mathbf{X'}_{a,b}$

$p \leftarrow length(\mathbf{X}_{a,b})$
for all $t \in [1,\ldots,p]$ **do**
  $\mathbf{X'}_{a,b}(t) \leftarrow$ NULL
  $\mathbf{Q} \leftarrow$ set of indices q such that $\mathbf{X}_{a,b}(q) = \{t, j\}$, for all j in view b
  $\mathbf{J}, \mathbf{V} \leftarrow sort\big(\mathbf{D}(\mathbf{Q}), \text{'increasing order'}\big)$ {$\mathbf{J}$ gets the indices, $\mathbf{V}$ the distances}
  if $\mathbf{V}(1) < \mathbf{V}(2) \cdot \sigma$ **then**
    $\mathbf{X'}_{a,b}(\mathbf{J}(1)) \leftarrow \{t, \mathbf{J}(1)\}$
    $\mathbf{X'}_{a,b}(\mathbf{J}(2)) \leftarrow$ NULL
  else
    $\mathbf{X'}_{a,b}(\mathbf{J}(1)) \leftarrow \{t, \mathbf{J}(1)\}$
    $\mathbf{X'}_{a,b}(\mathbf{J}(2)) \leftarrow \{t, \mathbf{J}(2)\}$
  end if
end for

Algorithm 2 : *W-weights* for two views a and b.

Input: $\mathbf{X}_{a,b}, \mathbf{D}_{a,b}$
Output: $\mathbf{W}_{a,b}$

$p \leftarrow length(\mathbf{X}_{a,b})$
for all $t \in [1,\ldots,p]$ **do**
  $\mathbf{W}_{a,b}(t) \leftarrow$ NULL
  $\mathbf{J} \leftarrow$ set of indices q such that $\mathbf{X}_{a,b}(q) = \{t, j\}$, for all j in view b
  $\mathbf{I} \leftarrow$ set of indices q such that $\mathbf{X}_{a,b}(q) = \{i, t\}$, for all i in view a
  if $cardinality\big(\mathbf{I}\big) == 1$ **then**
    $\mathbf{W}_{a,b}(\mathbf{J}) \leftarrow 1$
  else
    $\mathbf{W}_{a,b}(\mathbf{I}) \leftarrow \dfrac{\mathbf{D}(\mathbf{I})}{min\big(\mathbf{D}(\mathbf{I})\big)}$
  end if
end for

$$\hat{\mathbf{m}}_c^k = \frac{1}{m_a^{i\,\mathrm{T}}\left(T_{\cdot}^{\cdot 13} - x_b^j T_{\cdot}^{\cdot 33}\right)} \begin{bmatrix} m_a^{i\,\mathrm{T}}\left(T_{\cdot}^{\cdot 11} - x_b^j T_{\cdot}^{\cdot 31}\right) \\ m_a^{i\,\mathrm{T}}\left(T_{\cdot}^{\cdot 12} - x_b^j T_{\cdot}^{\cdot 32}\right) \end{bmatrix},$$

where the 3×3×3 trifocal tensor $\mathbf{T} = (T_t^{rs})$ encodes the relative motion among the views a, b and c. (Computed using the *point-line-point* method (Hartley and Zisserman 2000)). The projected position $\hat{\mathbf{m}}_c^k$ is compared to all segmented potential flaws $\mathbf{m}_c^k$ in the

Algorithm 3 : *Bidirectional* NNDR (bNNDR) criterion for two views a and b.

Input: $\mathbf{X}_{a,b}, \mathbf{D}_{a,b}$
Output: $\mathbf{X'}_{a,b}$
1: $p \leftarrow length(\mathbf{X}_{a,b})$
2: $\mathbf{W}_{a,b} \leftarrow$ *W-weights*$(\mathbf{X}_{a,b}, \mathbf{D}_{a,b})$ {by Algorithm **2**}
3: **for all** $t \in [1, \ldots, p]$ **do**
4: $\quad \mathbf{D'}_{a,b}(t) \leftarrow \mathbf{W}_{a,b}(t) \cdot \mathbf{D}_{a,b}(t)$
5: **end for**
6: $\mathbf{X'}_{a,b} \leftarrow NNDR(\mathbf{X}_{a,b}, \mathbf{D'}_{a,b})$ {by Algorithm **1**}

Algorithm 4 : *Bidirectional* NNDR (bNNDR) criterion for three views a, b, and c.

Input: $\mathbf{X}_{a,b,c}$
Output: $\mathbf{X'}_{a,b,c}$
1: $p \leftarrow length(\mathbf{X}_{a,b,c})$
2: **for all** view-pair $(x, y) \in \{(a, b), (a, c), (b, c)\}$ **do**
3: $\quad \mathbf{X}_{x,y} \leftarrow$ *bifocal matches*$(x, y, \mathbf{X}_{a,b,c})$
4: $\quad \mathbf{D}_{x,y}, \leftarrow$ *feature distances*$(\mathbf{X}_{x,y})$
5: $\quad \mathbf{W}_{x,y} \leftarrow$ *W-weights*$(\mathbf{X}_{x,y}, \mathbf{D}_{x,y})$
$\quad$ {Note: $length(\mathbf{X}_{x,y}) = length(\mathbf{D}_{x,y}) = length(\mathbf{W}_{x,y}) = p$}
6: **end for**
7: **for all** $t \in [1, \ldots, p]$ **do**
8: $\quad \mathbf{D'}_{a,b,c}(t) \leftarrow \mathbf{W}_{a,b}(t) \cdot \mathbf{D}_{a,b}(t) \cdot \mathbf{W}_{a,c}(t) \cdot \mathbf{D}_{a,c}(t) \cdot \mathbf{W}_{b,c}(t) \cdot \mathbf{D}_{b,c}(t)$
9: **end for**
10: $\mathbf{X'}_{a,b,c} \leftarrow NNDR(\mathbf{X}_{a,b,c}, \mathbf{D'}_{a,b,c})$

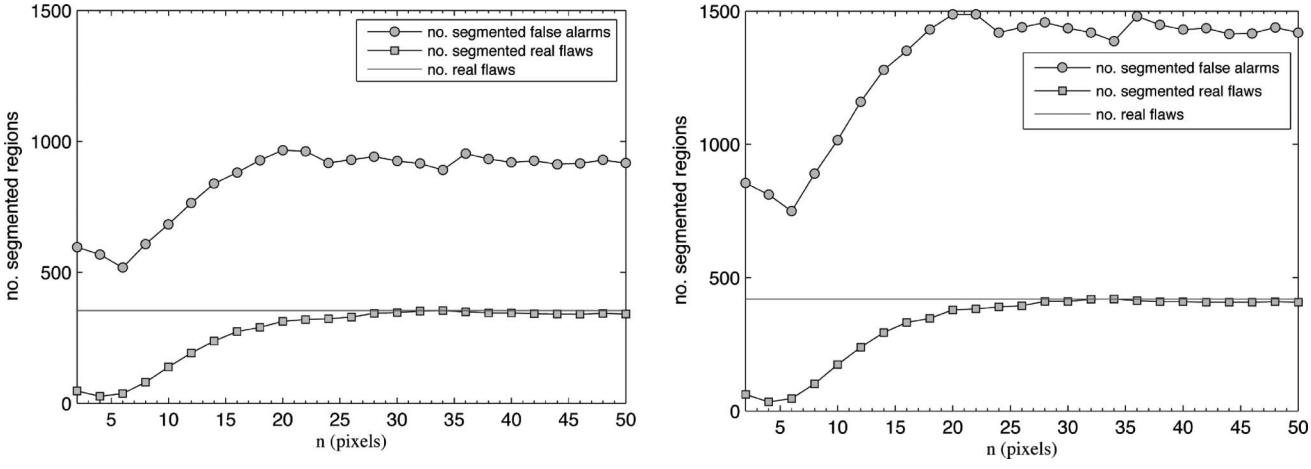

Figure 8. Influence of the kernel size $n \times n$ on the *structure removal* (SR) filter in the segmentation process. The larger n the more real flaws can be successfully segmented (a) in two views and (b) in three views. The solid line indicates the total number of real flaws present in the image sequences.

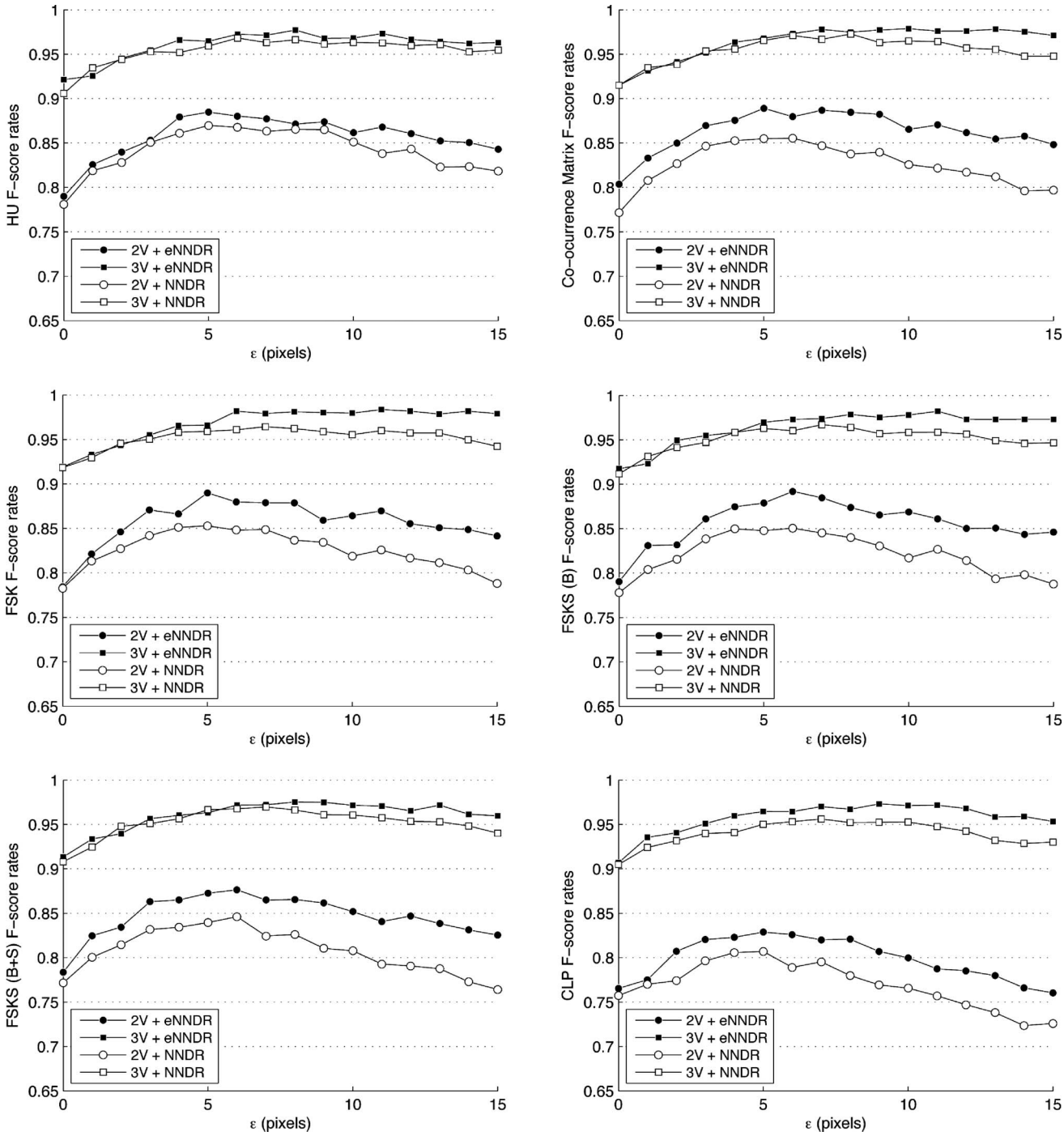

Figure 9. Performance comparison of the proposed two and three view inspection processes. The influence of the parameter ε is tested to obtain the geometric matches, as well as the NNDR and bNNDR criteria for feature analysis using the feature descriptors (from left to right, top to bottom): HU, Co-ocurrence, FSK, FSK(B), FSK(B + S), CLP (see Table 1).

third view c, and chooses as the corresponding flaw the one that satisfies

$$\|\hat{\mathbf{m}}_c^k - \mathbf{m}_c^k\| < \varepsilon \tag{3}$$

If condition (3) is fulfilled, as in the example of Figure 6(b), a geometric correspondence in three views has been found but it remains to be seen whether their respective feature vectors are also close to each other. If no segmented region in view c satisfies (3)

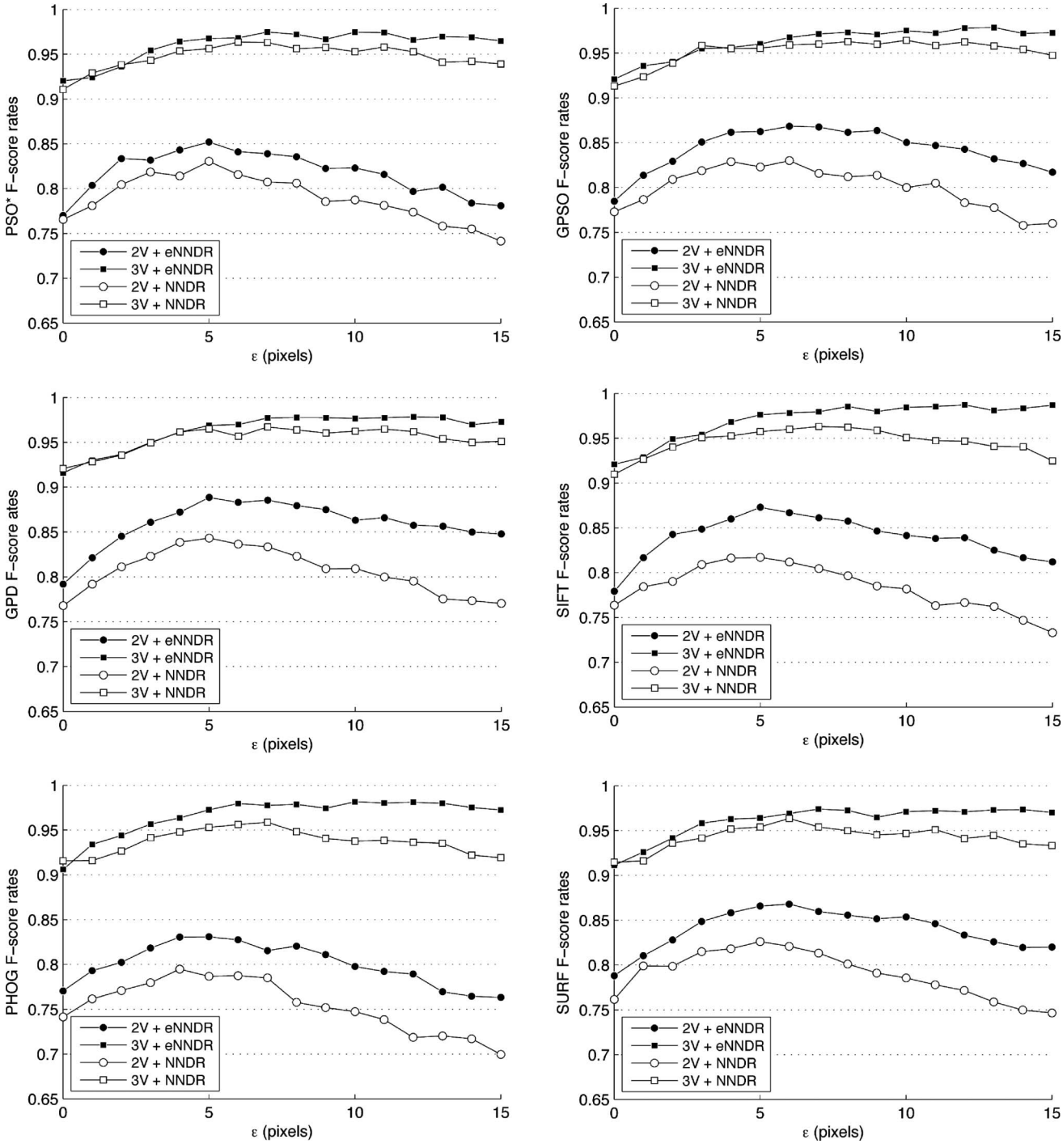

Figure 10. Performance comparison of the proposed two and three view inspection processes. The influence of the parameter ε is tested to obtain the geometric matches, as well as the NNDR and bNNDR criteria for feature analysis using the feature descriptors (from left to right, top to bottom): PSO*, GPSO, GPD, SIFT, PHOG, SURF (see Table 1).

correspondences $\mathbf{m}_a^i$ and $\mathbf{m}_b^j$ are regarded as false alarms.

In the two-view tracking process there are numerous false alarms that fulfill condition (3) and are considered potential flaw candidates. When using three views, that number greatly diminishes due to the extremely low probability that a false alarm would maintain its position in relation to the objects movement in three views. Let $\mathbf{X}_{a,b,c} \in \mathbf{Z}^{p\times 3}$ be an array with triplets $\{i, j, k\}$ that all fulfil condition (3). The system

filters out the wrong matches by analysing their featural characteristics with the adapted bNNDR criterion for three views described in Algorithm 4. The output array $\mathbf{X}'_{a,b,c}$ contains the correct triplets whose feature vectors match in all three views. The following section shows that this algorithm allows real flaws to be distinguished from false alarms with high accuracy. Although this methodology can be easily extended to process n views, three views suffice for the application considered in this paper.

4. Experimental results

It is now time to evaluate the performance of the proposed methodology for inspecting bottlenecks of empty wine bottles. The experiments utilised 120 colour image sequences. Each sequence consists of 3 views with a rotation angle of $\alpha = 15$ degrees between them. From the recorded images, the system extracts bottleneck sub-images of 1000×250 pixels. The number of real flaws per image fluctuates between 0 and 4 with an average of 2.8, and the number of false alarms per image fluctuates between 0 and 10 with an average of 9.5 per image. The area of the smallest flaw is around 9 pixels equivalent to 0.16 mm^2 on the bottle's surface. The performance is assessed considering two standard indicators (Olson and Delen 2008): $r = \frac{TP}{TP+FN}$ (recall) and $p = \frac{TP}{TP+FP}$ (precision). TP is the number of *true positives* or flaws correctly classified as such by the inspection system. FN is the number of *false negatives*, or existing real flaws, not detected. FP is the number of *false positives*, or flawless regions, that are incorrectly classified as defective. These two indicators can be cast in a unique measure $F_{SCORE} = \frac{2p \cdot r}{p+r}$ (Olson and Delen 2008). Ideally, one can expect $r = 100\%$, $p = 100\%$, and $F_{SCORE} = 1$. The following subsections evaluate several aspects of the proposed framework for detecting flaws in uncalibrated images of glass bottlenecks.

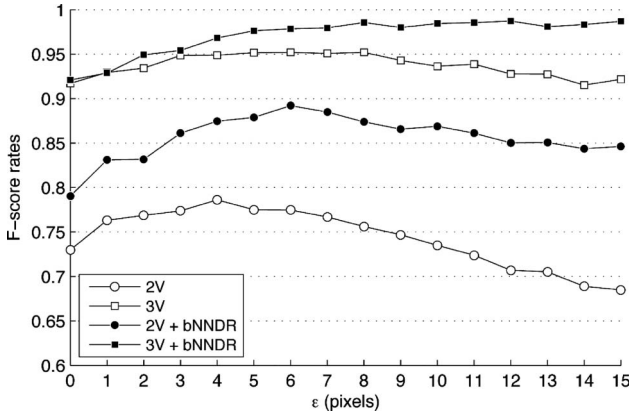

Figure 11. Performance comparison of inspection using only geometric constraints (2V and 3V) and including the proposed bNNDR criterion for feature analysis. In the latter case, feature descriptors FSKS(B) and SIFT are used in two and three views, respectively.

4.1. Evaluation of the segmentation process

The segmentation process described in Section 3.1 outputs a set of regions with potential flaws. This process has to be able to segment all real flaws present in the bottlenecks. Figure 8 shows how well this task performs as a function of the kernel size of the *structure removal* (SR) filter utilised to obtain a background image. The more uniform this image, the more real flaws are successfully extracted by the segmentation. However, the number of false alarms,

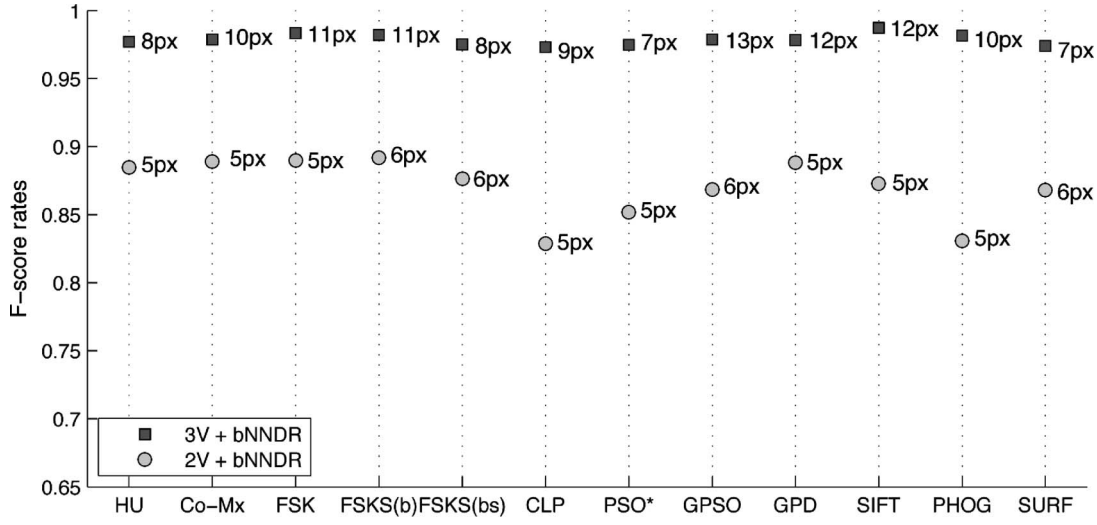

Figure 12. Best inspection performance running the bNNDR criterion for each feature descriptor. Optimal ε-values has been chosen.

i.e., regions that do not represent real flaws, also augment with increasing n. In the subsequent experiments we have set $n = 34$.

4.2. *Evaluation of the tracking processes*

The following examines the performance of the inspection methodology for detecting real flaws and discarding false alarms. The following denotes as 2V (two views) and 3V (three views) the inspection results obtained using only the geometric conditions (2) and (3) respectively. Similarly, 2V + *criterion* and 3V + *criterion* represent the inspection results obtained by further utilisation of one of the feature analysis criteria NNDR or bNNDR. Figure 9 and Figure 10 exhibit F-scores of the tracking processes in two and three views using all feature descriptors described in Table 1 considering both the NNDR criterion (Mikolajczyk and Schmid 2004) and the proposed *bidirectional* NNDR (bNNDR) criterion. The results are displayed as a function of the parameter ε that denotes the maximal distance (in pixels) at which one looks for geometric matches in two and three views, cf. conditions (1) and (2). Note that in all plots the three-view inspection process largely outperforms its two-view counterpart. The improvement introduced by our bNNDR criteria in contrast to the NNDR criteria is notable. These criteria are useful in resolving misleading *many-to-many* geometric matches (Figure 7).

The uncalibrated nature of the images can produce imprecision in the estimation of the fundamental matrices and trifocal tensors. Therefore it is sometimes necessary to use a larger parameter ε, as it is drawn in Figures 9 and 10. Although this can lead to the appearance of more misleading geometric matches, this problem is effectively overcome thanks to the utilisation of the feature analysis criteria. Figure 11

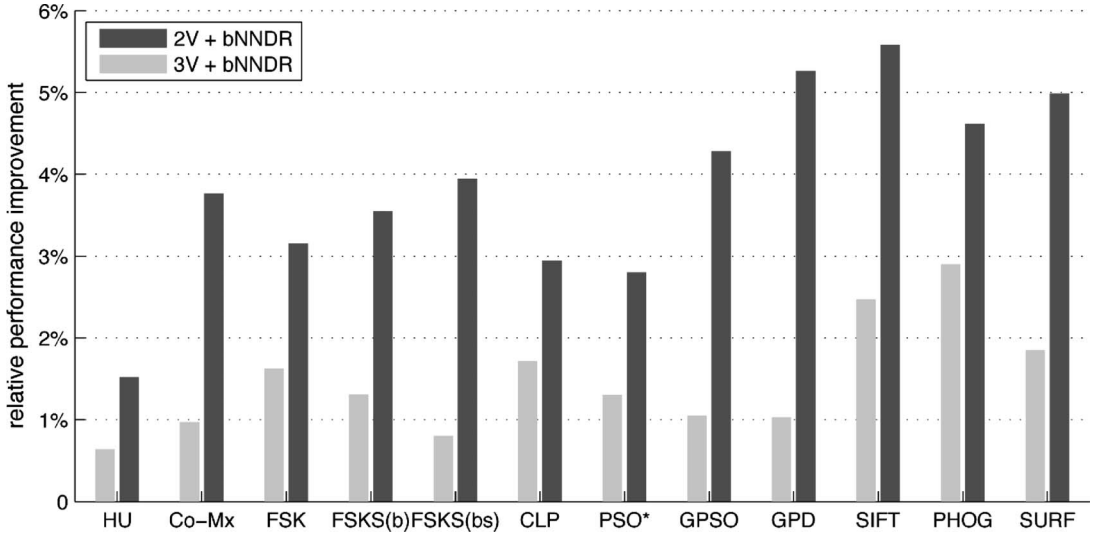

Figure 13. Mean relative performance improvement achieved by the proposed bNNDR criterion with respect to the NNDR criterion for each feature descriptor.

Table 2. Quantitative comparison of inspection systems for flaw detection in glass bottles. Our proposed methodology achieves the highest performance detecting flaws in the bottlenecks.

Inspected bottle part	Views	Tracking	TPR	FPR
Neck (Mery and Medina2004)	Single	No	85%	4%
Lips, Body, Bottom (Duan *et al.* 2007)	Single	No	97%	>1%
Lips (Wang *et al.* 2005)	Single	No	98%	0%
Body (Firmin *et al.* 1997, Hamad 1998)	Multiple	No	85%	2%
Lips, **Neck** (Ma *et al.* 2002)	Multiple	No	98%	2%
Body, Bottom (Shafait *et al.* 2004)	Multiple	No	100%	>1%
Neck (our method)	2V	Yes	99.9%	46.4%
	2V + bNNDR	Yes	99.9%	30.2%
	3V	Yes	99.1%	2.5%
	3V + bNNDR	Yes	**99.1%**	**0.9%**

shows the performance of the tracking algorithms when only geometric matches are sought in contrast to the performance obtained by additionally employing the proposed bNNDR criterion for feature analysis. It is clear that the latter case provides better results, especially when only two views are considered. Figure 12 displays performance using optimal ε-values for the geometric matches in combination with the bNNDR criterion with each feature descriptor. Figure 13 shows the relative performance improvement of the bNNDR criterion compared to the NNDR criterion.

Table 2 juxtaposes the inspection results with those from other inspection systems proposed in literature, indicating the usage of single or multiple images. This analysis includes all the processing stages for the detection of real flaws and the reduction of false alarms applied by means of the proposed inspection model. In a first stage, the algorithm processes each image of the sequence by means of a classic segmentation method, as was previously described. For each region, a set of feature descriptors is used to evaluate its performance independently. In this step 100% of the existing real flaws are detected, but unfortunately so is a high percentage of false alarms, constituting 100% of false alarms that must be reduced. In this stage of the process all the segmented regions (real flaws and false alarms) correspond to potential flaws for the tracking algorithm. Therefore the objective of the algorithm is to reduce the number of false alarms regions detected.

To evaluate the performance of the algorithm, a manual classification process was carried out with the purpose of evaluating if that potential flaw was a real flaw or a false alarm. Here different methods are compared in terms of the *true positive rate* $TPR = TP/(TP + FN)$ and the *false positive rate* $FPR = FP/(FP + TN)$, where TN is the number of segmented regions correctly classified as false alarms. An ideal inspection system would have 100% TPR and 0% FPR. It is important to mention that Table 2 corresponds to a quantitative comparison, since the other methods proposed in literature were tested on different images, types of bottles, and they inspect one or several bottle parts (lips, mouth, bottleneck, body, bottom). Nevertheless, the proposed method's results correspond to the most accurate reported in literature regarding the inspection of glass bottlenecks. This system emphasises the relevance of the combined use of geometry of multiple views and feature analysis of the potential flaws to distinguish between real flaws and false alarms effectively.

Concerning the computational aspects of the inspection system, the total time required to process three views was 1.3 s in average, running Matlab (7.0) code on a Pentium Centrino 2.0 GHz with Windows XP SP2. The time was spent as follows: Reading images from hard disk (34%), segmenting potential flaws (35%), geometric and featural analysis in three views (11%), and other Matlab internal operations (20%). This indicates that there is a lot of room for improvement in each of these tasks.

5. Conclusions

The use of multiple views does not mean that the problem is simpler. It means that there is a greater amount of information about the object or the evaluated scene. Therefore, decision making is more robust. In the case of automatic visual inspection the use of multiple views allows a reduction in the number of false alarms in a new classification process that operates in a manner similar to geometric tracking. Under this paradigm it is possible to increase the detection of real flaws because now a real flaw is visible in more than one view and at the same time reduce the false alarms because they are not visible in all views, mainly owing to the randomness of their relative positions.

This paper has two relevant contributions. First, it presented the prototype of an image acquisition system for capturing image sequences of glass bottlenecks using a single camera, where no camera calibration process is considered. The main novelty of this prototype is the placement of the illumination source inside the bottle, which greatly improves the quality of the acquired images, avoiding the intrinsic reflections produced by external light sources. Second, this paper introduced a novel methodology for inspecting glass bottlenecks using uncalibrated images. Our inspection system examines series of two and three images employing geometry of multiple views followed by a feature analysis stage to discriminate between real flaws and false alarms. This way, the system classifies as real flaws those that present similar characteristics in a set of images taken from different viewpoints. An important ingredient to achieve this goal was the introduction of a novel feature analysis criterion to resolve multiple geometric matches in different views. It can be considered as a bidirectional variant of the *nearest neighbour distance ratio* (NNDR) criterion proposed by Mikolajczyk and Schmid (2004). The term bidirectional has to do with how the algorithm increases the matching of two possible regions of similar properties (in this case real flaws), and at the same time decreases the number of false alarms in multiple views. It is necessary to point out that this is a generic correspondence algorithm that improves the performance of the NNDR algorithm. Regarding the performance, this inspection system, when tested on image sequences of wine glass bottles with real flaws,

obtained a true positive rate of 99.1% and a false positive rate of 0.9%.

An important characteristic of the proposed methodology for flaw detection is that no camera calibration is considered at all. This makes the proposed method suitable for applications where camera calibration is difficult or expensive to carry out. Moreover, this approach is generic in the sense that it can be used for the visual inspection of other manufactured objects as well.

Acknowledgements

M. Carrasco was partially supported by the *National Commission for Scientific and Technological Research* (CONICYT) under grant no. 21050185, and L. Pizarro was partially supported by the *German Academic Exchange Service* (DAAD) under grant A/05/21715.

References

Bay, H., 2008. SURF: Speeded up robust features. *Computer Vision and Image Understanding (CVIU)*, 110 (3), 346–359.

Bosch, A. and Zisserman, A.X.M., 2007. Representing shape with a spatial pyramid kernel. Paper presented at the *Proceedings of the 6th ACM international conference on Image and Video Retrieval (CIVR)*, Amsterdam, The Netherlands.

Canivet, M., Zhang, R.D., and Jourlin, M., 1994. Finish inspection by vision for glass production. *In*: Paper presented at the *Machine Vision Applications in Industrial Inspection II*, San Jose, CA, USA.

Carrasco, M. and Mery, D., 2006. Automated visual inspection using trifocal analysis in an uncalibrated sequence of images. *Materials Evaluation*, 64 (9), 900–906.

Carrasco, M. and Mery, D., 2010. Automatic multiple view inspection using geometrical tracking and feature analysis in aluminum wheels. *Machine Vision and Applications*. In press. DOI: 10.1007/s00138-010-0255-2.

Castleman, K., 1996. *Digital image processing*. New Jersey: Prentice-Hall.

Chen, Z., 2000. A robust algorithhm to estimate the fundamental matrix. *Pattern Recognition Letters*, 21, 851–861.

Chin, R. and Harlow, C., 1982. Automated Visual Inspection: A survey. *IEEE Transactions on Pattern Analysis and Machine Intelligence*, 4 (6), 557–573.

Chung, Y.K. and Kim, K.H., 1998. Automated visual inspection system of automobile doors and windows using the adaptive feature extraction. Paper presented at the *Second International Conference on Knowledge-Based Intelligent Electronic Systems, KES98*, Adelaide, Australia.

Drury, C.G., Saran, M., and Schultz, J., 2004. Temporal effects in aircraft inspection: What price vigilance research? Paper presented at the *Proceedings of the Human Factors and Ergonomics Society 48th Annual Meeting*, Santa Monica, CA.

Duan, F., Wang, Y.-N., Liu, H.-J., and Li, Y.-G., 2007. A machine vision inspector for beer bottle. *Engineering Applications of Artificial Intelligence*, 20 (7), 1013–1021.

Firmin, C., Hamad, D., Postaire, J.G., and Zhang, R.D., 1997. Gaussian neural networks for bottles inspection: a learning procedure. *International Journal of Neural Systems*, 8 (1), 41–46.

Flusser, J. and Suk, T., 1993. Pattern recognition by affine moment invariants. *Pattern Recognition*, 26 (1), 167–174.

Flusser, J., Suk, T., and Saic, S., 1996. Recognition of images degraded by linear motion blur without restoration. *Computing Supplement*, 11, 37–51.

Hamad, D., 1998. Neural Networks inspection system for glass bottles production: A comparative study. *International Journal of Pattern Recognition and Artificial Intelligence*, 12 (4), 505–516.

Haralick, R., Shanmugam, K., and Dinstein, I., 1973. Textural features for image classification. *IEEE Transactions on Systems, Man, and Cybernetics, SMC-3*, (6), 610–621.

Hartley, R. and Zisserman, A., 2000. *Multiple view geometry in computer vision*. Cambridge, UK: Cambridge University Press.

Hu, M.K., 1962. Visual pattern recognition by moment invariants. *IRE Trans Info Theory, IT*, (8), 179–187.

Hui-Fuang, N., 2006. Automatic thresholding for defect detection. *Pattern Recognition Letters*, 27 (14), 1644–1649.

Jacob, R., 2004. Improving inspector's performance and reducing errors – general aviation inspection training systems (Gaits). Paper presented in *Proceedings of the Human Factors and Ergonomics Society Annual Meeting*, Santa Monica, CA.

Jarvis, J.F., 1980. Visual inspection automation. *Computer*, 13 (5), 32–38.

Katayama, K., Ishikura, T., Kodoma, Y., Fukuchi, H., and Fujiwara, A., 2008. USA Patent No.

Kumar, A., 2008. Computer-vision-based fabric defect detection: a survey. *IEEE Transactions on Industrial Electronics*, 55 (1), 348–363.

Liao, T., 2003. Classification of welding flaw types with fuzzy expert systems. *Expert Systems with Applications*, 25 (1), 101–111.

Linhari, E. and Obac, V., 2005. Methodology for classification of images based on the characteristics of a new interpretation of Shannon's entropy. *Wood Science Technology*, 39 (2), 113–128.

Lowe, D.G., 2004. Distinctive image features from scale-invariant keypoints. *International Journal of Computer Vision*, 60 (2), 91–110.

Ma, H.M., Su, G.D., and Ni, J.Y.W.Z., 2002. A glass bottle defect detection system without touching. Paper presented at the *International Conference on Machine Learning and Cybernetics*.

Malamas, E., Petrakis, E.G., and Zervakis, M., 2003. A survey on Industrial Vision Systems, applications and tools. *Image and Vision Computing*, 21 (2), 171–188.

Mamic, G. and Bennamoun, M., 2000. *Automatic flaw detection in textiles using a Neyman-Pearson detector*. Paper presented at the *Proceedings of the international Conference on Pattern Recognition (ICPR)*, Washington, DC.

Marchand, E., 2007. Control camera and light source positions using image gradient information. Paper presented at the *IEEE International Conference on Robotics and Automation (ICRA)*, Rome, Italy.

Martin, J., 2005. *BASIC stamp syntax and reference manual*. Parallax, USA.

Mery, D., 2003. Crossing line profile: a new approach to detecting defects in aluminium castings. *Lecture Notes in Computer Science*, 2749, 725–732.

Mery, D. and Filbert, D., 2002. Automated flaw detection in aluminum castings based on the tracking of potential defects in a radioscopic image sequence. *IEEE Transactions on Robotics and Automation*, 18 (6), 890–901.

Mery, D. and Medina, O., 2004. Automated visual inspection of glass bottles using adapted median filtering. *Lecture Notes in Computer Science*, 3212, 818–825.

Mikolajczyk, K. and Schmid, C., 2004. A performance evaluation of local descriptors. *IEEE Transactions on Pattern Analysis and Machine Intelligence*, 27 (10), 1615–1630.

Mindru, F., 2004. Moment invariants for recognition under changing viewpoint and illumination. *Computer Vision and Image Understanding*, 94 (1–3), 3–27.

Mital, A., Govindaraju, M., and Subramani, B., 1998. A comparison between manual and hybrid methods in parts inspections. *Integrated Manufacturing Systems*, 9 (6), 344–349.

Olson, D.L. and Delen, D., 2008. *Advanced data mining techniques*. Berlin: Springer.

Parker, J., 2000. Defect in glass and their origin. Paper presented at the *First Balkan Conference on Glass Science and Technology*, Vollos, Greace, University of Thessaly.

Pizarro, L., Mery, D., Delpiano, R., and Carrasco, M., 2008. Robust automated multiple view inspection. *Pattern Analysis and Applications*, 11 (1), 21–32.

Shafait, F., Imran, S., and Klette-Matzat, S., 2004. Fault detection and localization in empty water bottles through machine vision. Paper presented at the *Emerging Technology Conference (E-Tech)*.

Sidibe, D., Montesinos, P., and Janaqi, S., 2007. Fast and robust image matching using contextual information and relaxation. Paper presented at the *2nd International Conference on Computer Vision Theory and Applications, VISAPP*, Barcelona, Spain.

Vazquez, P.P., 2007. Automatic light source placement for maximum visual information recovery. *Computer Graphics Forum*, 26 (2), 143–156.

Wang, J. and Asundi, A., 2000. A computer vision system for wineglass defect inspection via Gabor-filter-based texture features. *Information Sciences*, 127 (3–4), 151–171.

Wang, Y.N., H.-J.L., and Duan, F., 2005. A bottle finish inspect method based on fuzzy support vector machines and wavelet transform. Paper presented at the *International Conference on Machine Learning and Cybernetics*.

Yan, T.S. and Cui, D.W., 2006. The method of intelligent inspection of product quality based on computer vision. Paper presented at *the Proceedings of the 7th International Conference on Computer-Aided Industrial Design and Conceptual Design (CAIDCD)*, Hangzhou, China.

Yepeng, Z., Yuezhen, T., and Zhiyong, F., 2007. Application of digital image process technology to the mouth of beer bottle defect inspection. Paper presented at the *Proceedings of the 8th International Conference on Electronic Measurement and Instruments*.